

Bus Admittance Matrix Revisited: Is It Outdated on Modern Computers?

Hantao Cui, *Senior Member, IEEE*

Abstract—Bus admittance matrix is widely used in power engineering for modeling networks. Being highly sparse, it requires fewer CPU operations when used for calculations. Meanwhile, sparse matrix calculations involve numerous indexing and scalar operations, which are unfavorable to modern processors. Without using the admittance matrix, nodal power injections and the corresponding sparse Jacobian can be computed by an element-wise method, which consists of a highly regular, vectorized evaluation step and a reduction step. This paper revisits the admittance matrix from the computational performance perspective by comparing it with the element-wise method. Case studies show that the admittance matrix method is generally slower than the element-wise method for grid test cases with thousands to hundreds of thousands of buses, especially on CPUs with support for wide vector instructions. This paper also analyzes the impact of the width of vector instructions and memory speed to predict the trend for future computers.

Index Terms—Bus admittance matrix, sparse matrix, high-performance computing, vectorization, single-instruction multiple data (SIMD).

I. INTRODUCTION

BUS admittance matrix (also known as admittance matrix, \mathbf{Y} matrix, or \mathbf{Y}_{bus}) is ubiquitous in power engineering for network modeling [1]. The bus admittance matrix reduces a power grid with n_b buses and n_l lines into an n_b -port network by relating bus current injections to bus voltages. In realistic systems, a bus is only connected to a few other buses, thus the admittance matrix is highly sparse. By adopting sparse matrix techniques, calculations based on \mathbf{Y}_{bus} requires significantly less memory and arithmetic operations, making it superior to the then-popular impedance matrix method [2].

In many power systems studies such as power flow and stability simulations, \mathbf{Y}_{bus} is used to calculate bus power injections, as well as the Jacobian matrix that contains the partial derivatives of injections concerning voltages and angles. The computational performance to obtain network injections and Jacobians is highly relevant because their computation time is only second to solving sparse linear equations. Over the past decades, the central processing units (CPUs) in computers have seen significant upgrades and shifted growth paradigms [3], but not all computations can benefit equally. Calculations using \mathbf{Y}_{bus} require sparse matrix-vector products, where both the sparse matrix and vector are composed of complex numbers. Such calculations are non-atomic to processors, thus the performance gain depends on multiple factors and remains to be investigated.

Various techniques have been developed for modern CPUs with the primary goal to reduce latency [4], [5]. In the early

1980s, arithmetic calculations were already faster than accessing data in memory, thus caches were added to CPU chips. Instruction pipelining was later added to execute multiple, similar, and independent instructions in different stages of completion. In the 90s, branch prediction and out-of-order execution were added for relaxing dependent calculation. With a probability of success, dependent calculations can be executed in parallel. Another relevant technique is vector instruction known as single-instruction multiple data (SIMD), which allows the processing of data in packs. To benefit from these techniques and achieve high performance, the rule of thumb is to design algorithms and data structures that exhibit regularity [6], which translates to predictability for compilers and the hardware.

The sparse \mathbf{Y}_{bus} method is not unique for network injection calculation. An alternative method is termed the “element-wise method” (or the vectorized method), which calculates the element-wise power injections to form branch-power vectors. Power injections into the line terminal are then summed up at the connected buses to obtain the bus-wise power injections [7], [8]. The equations for the element-wise method are not unfamiliar, but the method is often dismissed because typical power grids have more lines than buses. Nevertheless, calculations in the element-wise method exhibit repetitiveness, namely, the same calculations on different data, which may be favored by modern CPUs.

This paper aims to provide a high-performance computing perspective on the \mathbf{Y}_{bus} method and the element-wise method for *a)* bus power injection calculation and *b)* sparse Jacobian matrix formulation. The method formulations, optimized implementations, data access patterns, and computational complexity are presented. While this work does not study the solution of equations, the formulated equations and sparse Jacobians can be readily interfaced with efficient solvers. Rather, the objective is to identify the method with higher performance and understand its scalability limitations on modern CPUs.

The main contribution of this paper is the finding that the \mathbf{Y}_{bus} method is generally slower than the element-wise method for large-scale power systems. This finding is based on rigorous implementation and benchmarks of highly optimized implementations. All benchmarks performed on recent Intel and Apple platforms support the observation, using test systems ranging from 14 to 82,000 buses and more. Also, the reasons why the \mathbf{Y}_{bus} method is trailing are discussed. Further, the impact of CPU features and memory performance are analyzed to assess the scalability promise of the two methods.

This paper is organized as follows: Section II discusses the fundamental formulations of the \mathbf{Y}_{bus} method and element-wise method. Section III briefly introduces CPU features and

computer architecture relevant for result interpretation. Section IV discusses data structures, computation steps, and implementation techniques for high performance. Section V presents the benchmark data to compare different CPU generations across different architectures. Section VI concludes the finding and predicts the scalability of two methods on future hardware.

II. METHOD FORMULATIONS

This section discusses the formulations to calculate network power injections and Jacobians.

A. \mathbf{Y}_{bus} Method

The complex power injections are calculated by

$$\mathbf{S} = \mathbf{V} \cdot (\mathbf{Y}_{bus} \mathbf{V})^* \quad (1)$$

where \mathbf{S} and \mathbf{V} are two complex-number vectors, respectively, for power injections and voltage phasors.

The corresponding Jacobian matrix is given by

$$\mathbf{J} = \begin{bmatrix} \mathbf{J}_{11} & \mathbf{J}_{12} \\ \mathbf{J}_{21} & \mathbf{J}_{22} \end{bmatrix} = \begin{bmatrix} \text{Re}(\partial \mathbf{S} / \partial \boldsymbol{\theta}) & \text{Re}(\partial \mathbf{S} / \partial \mathbf{V}) \\ \text{Im}(\partial \mathbf{S} / \partial \boldsymbol{\theta}) & \text{Im}(\partial \mathbf{S} / \partial \mathbf{V}) \end{bmatrix} \quad (2)$$

where the derivative sub-matrices are calculated by [9]

$$\frac{\partial \mathbf{S}}{\partial \boldsymbol{\theta}} = j \cdot \text{diag}(\mathbf{V}) [\text{diag}(\mathbf{I}_c^*) - (\mathbf{Y}_{bus} \text{diag}(\mathbf{V}))^*] \quad (3)$$

$$\frac{\partial \mathbf{S}}{\partial \mathbf{V}_m} = \text{diag}(\mathbf{I}_c^* \cdot e^{j\theta}) + \text{diag}(\mathbf{V})(\mathbf{Y}_{bus} \text{diag}(e^{j\theta}))^* \quad (4)$$

Although (3) and (4) are compact, they are not of top efficiency as both require multiple sparse-sparse multiplications. Section III will discuss an efficient two-pass algorithm to simultaneously compute the two derivative matrices.

B. Element-wise Method

Consider a transmission line or a two-winding transformer whose off-nominal tap ratio and phase shift $me^{j\phi}$ is applied at the primary side. The complex power injections S into the two terminals, h and k , are given by

$$S_{hk} = v_h^2 \frac{(y_h + y_{hk})^*}{m^2} - v_h v_k \frac{y_{hk}^*}{m} e^{j(\theta_h - \theta_k - \phi)} \quad (5)$$

$$S_{kh} = -v_h v_k \frac{y_{hk}^*}{m} e^{-j(\theta_h - \theta_k - \phi)} + v_k^2 (y_k + y_{hk})^* \quad (6)$$

where y_h are the shunt admittance (including transformer core losses and magnetizing reactance) at the h terminal, y_k is the shunt admittance at the k terminal, y_{hk} is the series admittance, v_h and v_k are the voltage magnitudes, and θ_h and θ_k are the voltage phase angles of buses h and k .

The power injection into bus i can be obtained by adding up all the injections from connected lines:

$$S_i = \sum_{t=1}^{n_b} S_{it}, (i, t) \in L \quad (7)$$

where t is the other terminal of an existing line that connects buses i and t , and L is the set of lines denoted by bus pairs. Each of (5) and (6) needs to be evaluated for n_l times, and (7) requires up to $2n_l$ additions.

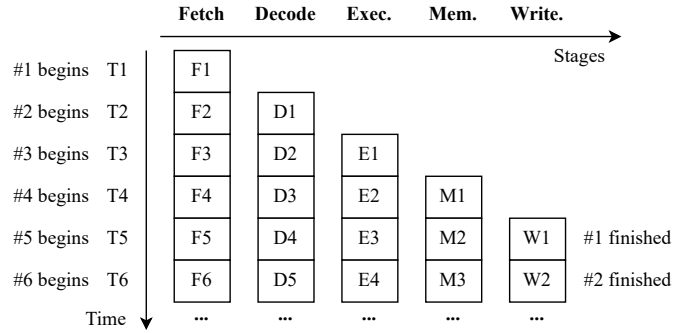


Fig. 1. Illustration of pipelining six instructions in a five-stage pipeline.

To obtain the sparse Jacobian matrix, one first calculates the non-zero Jacobian entries and then assemble them into a sparse matrix. The four power injection equations (P_h , Q_h , P_k and Q_k) can be obtained from (5) and (6). Taking the partial derivative of the four equations with respect to four variables (v_h , θ_h , v_k , and θ_k) yields 16 expressions. All 16 expressions need to be evaluated for all n_l lines to obtain the complete Jacobian elements. Given a large number of Jacobian expressions and the number of lines, this method is perceived as having high computational complexity.

III. MODERN CPU FEATURES

This section will walk through the features of modern CPUs to provide a fundamental understanding of comparing the two methods. These features include *a*) cache and prefetch, *b*) single-instruction multiple-data (SIMD) vectorization, *c*) pipelining and branch prediction. All these features serve one goal: to reduce the overall latency.

Modern CPUs have multiple levels of on-chip cache. These caches are made of static random-access memory (SRAM) so is faster to access than memory, which is made of dynamic random-access memory (DRAM). For example, an Intel Core i9-12900K has three levels of cache, namely, L1, L2, and L3, with respective sizes of 80 KB (per core), 1.25 MB (per core), and 30 MB (total). The time to access the three levels of cache is around 1 ns, 4 ns, and 40 ns, compared with a typical memory access time of 80 ns. If the requested data is in the cache, the access is a “cache hit”. Otherwise, it is a “cache miss” and will incur time to access the memory.

To utilize the on-chip cache and improve the cache hit rate, “prefetch” is used to preemptively load data from memory to cache. Prefetch is accomplished by both the CPU hardware and the compiler, which may insert prefetch instructions into the machine code. Generally, data prefetch for an algorithm will have a higher success rate if the algorithm access data in a more regular manner, such as visiting a memory block linearly. Conversely, if the data locations can only be determined at run time, prefetch success will likely decrease.

To reduce the number of instruction cycles for the same computations, a single-instruction multiple-data (SIMD) instruction set is introduced. SIMD instructions in the x86 platform include the Advanced Vector eXtension (AVX) instructions, which can perform simultaneous arithmetic operations

on four to eight double-precision floating points, using AVX2 and AVX512, respectively. To utilize SIMD, data operands need to be in the cache and ready to be loaded into vector registers. On the other hand, using SIMD will add overhead to calculations that are done on scalars with mixed memory access. In such cases, compilers will avoid generating SIMD instructions but instead use scalar operations.

Another relevant technique is instruction pipelining. Multiple stages are needed to execute an instruction, including fetch, decode, execute, memory access, and register write-back. Each stage is performed by a part of the CPU. Pipelining aims to keep all parts busy while executing multiple instructions. Fig. 1 illustrates the execution of six instructions in a five-stage pipeline. The first instruction takes T1 to T5 to complete. Starting from T6, each instruction will only take one time unit.

Although pipelines are efficient once warmed up, there is a downside. If one instruction needs to be changed within the pipeline, the pipeline will stall and needs to be flushed. Programs with `if-else` statements, for example, will likely introduce instruction changes due to jumping. Modern x86 processors have long pipelines, so for remediation, a branch prediction mechanism is introduced. If the prediction is correct, the pipeline can continue, and only a few cycles will be wasted. Otherwise, the time penalty will be much greater.

In summary, improving the cache hit rate, utilizing SIMD as much as possible, and reducing instruction changes will improve the performance of a program. As alluded to before, algorithms with a regular data storage and access pattern will improve prefetch and improve the cache hit rate. Also, programs with fewer conditional jumps will have better pipeline performance. These metrics will be utilized to qualitatively assess the efficiency of the \mathbf{Y}_{bus} and element-wise method.

IV. DATA STRUCTURE, STEPS, AND IMPLEMENTATIONS

This section presents sufficient details on the data structure, computation steps, and implementations that are crucial for a rigorous assessment of the two methods.

A. Data Structure

1) \mathbf{Y}_{bus} method: The prominent data structure for storing \mathbf{Y}_{bus} is the sparse matrix technique, which is comprehensively covered in the literature [10], [11]. The most common sparse formats to store \mathbf{Y}_{bus} are Compressed Sparse Column (CSC) and Compressed Sparse Row (CSR), and a trade-off exists between them. The CSR format is faster than CSC for sparse matrix-vector product operation but slower for factorization. If \mathbf{Y}_{bus} is in CSR, the resultant \mathbf{J} will be in CSR by default. Then, \mathbf{J} will need to be converted to CSC every time to interface with fast solvers like KLU [12]. As a result, it is more common to store \mathbf{Y}_{bus} and \mathbf{J} in the CSC format.

2) *Element-wise method*: The element-wise method does not require special data structures besides the array. To facilitate SIMD and pipelining, the same parameter or variable of all device instances is stored in a one-dimensional array. For example, an array \mathbf{v}_h will hold the sending-end voltage magnitudes of all lines. The data structure guarantees that all elements of \mathbf{v}_h are in contiguous memory.

The contiguous-memory requirement is also applied to the arrays of complex numbers. That is, the real and imaginary parts of complex numbers are stored in two separate arrays with an element type of floating point numbers. Also, one can separate the real power from reactive power in (5) and (6) so that no complex-valued arrays are needed.

B. \mathbf{Y}_{bus} Method: Computation Steps and Algorithms

1) *Power injection computation*: The following steps are performed in order to calculate the power injections:

- 1) Update the complex arrays $\mathbf{U} = e^{j\theta}$ and $\mathbf{V} = \mathbf{V}_m \cdot \mathbf{U}$
- 2) Calculate sparse matrix-vector product $\mathbf{I}_{bus} = \mathbf{Y}_{bus} \mathbf{V}$
- 3) Calculate two vector product $\mathbf{V} \cdot \mathbf{I}_{bus}^*$

where θ is the array of voltage phase angles, \mathbf{V}_m is the array of voltage magnitudes, and \mathbf{I}_{bus} is the array of current injections.

Steps 2 and 3 favor different data structures for \mathbf{V} for performance. For Step 2, the access into \mathbf{V} is random, which depends on the current column index of the non-zero element in \mathbf{Y}_{bus} . Placing together the real and imaginary parts of each complex element in \mathbf{V} will enable the retrieval of two values in one access. For Step 3, storing the real and imaginary parts of \mathbf{V} and \mathbf{I}_{bus} separately and linearly will enable SIMD support with improved pipeline efficiency. This conflict is fundamental and can only be alleviated by copying memory, which will incur overhead.

2) *Jacobian calculation*: A two-pass algorithm [13] is adopted to compute $\partial \mathbf{S} / \partial \theta$ and $\partial \mathbf{S} / \partial \mathbf{V}_m$ simultaneously and reuse intermediate values. This method observes the sparsity patterns of \mathbf{J} and \mathbf{Y}_{bus} . That is, calculations in (3) and (4) only involves the product of \mathbf{Y}_{bus} by diagonal matrices and the addition (or subtraction) of diagonal matrices. Since these operations will not introduce non-zero elements at locations where the corresponding \mathbf{Y}_{bus} element is zero, the Jacobians $d\mathbf{S}/d\theta$ and $d\mathbf{S}/d\mathbf{V}_m$ will have the same sparsity pattern as \mathbf{Y}_{bus} . More precisely, the locations of nonzeros in the Jacobians are subsets of the nonzeros in \mathbf{Y}_{bus} because some values may become zeros. Nonetheless, these small numbers of zeros can be stored to reuse the sparsity pattern of \mathbf{Y}_{bus} .

Algorithm 1 adopted from [14] presents the pseudo-code for the two-pass method for CSC sparse matrix. In the inputs, \mathbf{Y}_p , \mathbf{Y}_i and \mathbf{Y}_v are the column pointers, row indices, and nonzeros of the CSC storage of \mathbf{Y}_{bus} , \mathbf{I}_{bus} is the array for bus current injections. In the initialization phase, copying the non-zero values of \mathbf{Y}_{bus} to that of $d\mathbf{S}/d\theta$ and $d\mathbf{S}/d\mathbf{V}_m$ only involve linear memory access and is thus rapid. The first pass computes the \mathbf{Y}_{bus} -vector product in (3) and (4), and the second pass computes the remainder.

The two-pass method is more efficient than directly performing sparse matrix multiplications because

- 1) Memory allocation for sparse matrices is avoided due to the reuse of sparsity pattern.
- 2) Memory access to the non-zero values of $d\mathbf{S}/d\theta$ and $d\mathbf{S}/d\mathbf{V}_m$ are linear, thus data are more likely to have been prefetched to cache.

Also, note that a slightly more efficient version can be obtained for CSR-stored \mathbf{Y}_{bus} . Since many sparse linear solvers only support the CSC format, a CSR-to-CSC conversion will

Algorithm 1 Two-pass method for Jacobian using CSC

```

1: INPUT:  $\mathbf{Y}_p, \mathbf{Y}_i, \mathbf{Y}_v, d\mathbf{S}_\theta, d\mathbf{S}_V, \mathbf{I}_{bus}, \mathbf{V}, \mathbf{U}$ 
2: INITIALIZE:
3:    $\mathbf{I}_{bus} = 0, d\mathbf{S}_\theta.nzval .= \mathbf{Y}_v, d\mathbf{S}_V.nzval .= \mathbf{Y}_v$ 
4: PASS 1: for  $j = 1 : n_b$  ( $j$  is column index)
5:   for  $k = \mathbf{Y}_p[j] : (\mathbf{Y}_p[j+1] - 1)$  ( $k$  is  $j$ 's index range)
6:      $\mathbf{I}_{bus}[\mathbf{Y}_i[k]] += \mathbf{Y}_v[k] * \mathbf{V}[j]$ 
7:      $d\mathbf{S}_\theta.nzval[k] \times = \mathbf{V}[j]$ 
8:      $d\mathbf{S}_V.nzval[k] \times = \mathbf{U}[j]$ 
9:   end for  $k$ 
10: end for  $j$ 
11: PASS 2: for  $j = 1 : n_b$ 
12:   for  $k = \mathbf{Y}_p[j] : (\mathbf{Y}_p[j+1] - 1)$ 
13:      $i = \mathbf{Y}_i[k]$  ( $i$  is element  $k$ 's row number)
14:      $d\mathbf{S}_V.nzval[k] = \mathbf{V}[i] \times (d\mathbf{S}_V[K])^*$ 
15:     if  $i == j$ 
16:        $d\mathbf{S}_\theta.nzval[k] -= \mathbf{I}_{bus}[j]$ 
17:        $d\mathbf{S}_V.nzval[k] += (\mathbf{I}_{bus}[j])^* \times \mathbf{U}[j]$ 
18:     end if
19:      $d\mathbf{S}_\theta.nzval[k] = (1im) \times (d\mathbf{S}_\theta.nzval[k])^* \times \mathbf{V}[i]$ 
20:   end for  $k$ 
21: end for  $j$ 
22: RETURN:  $d\mathbf{S}_\theta, d\mathbf{S}_V$ 

```

be required at every step. The overhead of the conversion may out-weight the gain from using the CSR format.

3) *Jacobian matrix assembly*: The \mathbf{J} matrix with real values can be obtained by concatenation as given in (2), but sparse matrix concatenation is slow due to index sorting and memory allocation every time two sub-matrices are concatenated.

Algorithm 2 is proposed to facilitate rapid assembly of the real and imaginary parts of the complex Jacobians into \mathbf{J} , which is of the size $2n_b \times 2n_b$. With pre-allocated sparsity pattern for \mathbf{J} , the assembly operation is essentially copying the derivative elements to proper locations in \mathbf{J} . Since the sparsity patterns do not change, one can pre-calculate the indexing arrays \mathbf{P}_{xy} into \mathbf{J} 's non-zeros for corresponding sub-matrices.

Algorithm 2 is generalized for cases where all non-zeros of \mathbf{J}_{xy} exist in \mathbf{J} but not necessarily the other way. For a basic power flow calculation, each sub-matrices will have identical sparsity pattern to \mathbf{Y}_{bus} . This may not be the case when series devices other than lines and transformers (such as TCSC) exist. Algorithm 2 is thus designed to obtain the indices based on matching row and column coordinates.

Using the pre-calculated indices, the Jacobian submatrices can be rapidly copied by $\mathbf{J}.nzval[\mathbf{P}_{xy}] .= \mathbf{J}_{xy}.nzval$. This method is efficient because

- 1) no random access to the sparse matrix \mathbf{J} is needed. Time is thus saved by avoiding index look-ups,
- 2) the memory copy operations visit the sub-matrix non-zeros linearly, which improves cache performance.

C. Element-wise Method Computation Steps

1) *Vectorized calculation*: The element-wise method does not require sophisticated algorithms for calculation. The principle of the element-wise method is to separate CPU-bound

Algorithm 2 Obtain indices to write to sparsity pattern

```

1: INPUT:  $\mathbf{J}_p, \mathbf{J}_i, \mathbf{Y}_{row}, \mathbf{Y}_{col}, \mathbf{P}_{xy}$  where  $x, y \in (1, 2)$ 
2: INITIALIZE:
3:    $\mathbf{P}_{xy} .= 0$  where  $x, y \in (1, 2)$ 
4: LOOP FOR  $\mathbf{P}_{xy}$ : for  $i = 1 : \text{length}(\mathbf{Y}_{col})$ 
5:    $c_{ol} = \mathbf{Y}_{col}[i] + (y - 1) * n_b$ 
6:    $r_{ow} = \mathbf{Y}_{row}[i] + (x - 1) * n_b$ 
7:   for  $k = \mathbf{J}_p[c_{ol}] : (\mathbf{J}_p[c_{ol} + 1] - 1)$ 
8:     if  $\mathbf{J}_i[k] == r_{ow}$ 
9:        $\mathbf{P}_{xy}[i] = k$ ; break;
10:    end if
11:  end for  $k$ 
12: end for  $i$ 
13: RUN the loop with  $(x, y) = (1, 1), (1, 2), (2, 1),$  and  $(2, 2)$ 

14: RETURN:  $\mathbf{P}_{11}, \mathbf{P}_{12}, \mathbf{P}_{21}, \mathbf{P}_{22}$ 

```

vectorized evaluations from memory-bound operations and maximize SIMD utilization for the former. Since all parameters and variables are stored in arrays of an equal length, the evaluation of all expressions for the same device can be packed in the same loop, in which the same index is used to access the arrays. An illustration of the calculation loop is given in Listing 1,

```

1 for m in 1:n_line
2   Ph[m] = vh[m] * (vh[m] * itap2ghghk[m] - ...)
3   Pk[m] = vk[m] * (vk[m] * ghk[m] - ...) ...
4 end

```

Listing 1. Illustration of element-wise power injection calculation. Part of the expressions is omitted for brevity.

where all constants, such as $itap2ghghk = (g_h + g_{hk})/T_{ap}^2$, are calculated once ahead of time.

There are three benefits of element-wise evaluations:

- 1) the same parameters and variables are used in multiple expressions. As a result, cached values may be reused.
- 2) since the expressions across devices are homogeneous, the compiler can generate SIMD instructions to simultaneously evaluate one expression for multiple instances.
- 3) no branch exists in the calculation code, so the execution pipeline can be sustained.

After calculating the line-wise power injections, the bus-wise power injections are calculated using (7). This step is termed "reduction" as it reduces the number of injections from n_l to n_b . Given that multiple lines can connect to the same bus, each reduction involves three operations: load, add, and store. Also, for a given order of lines, their connected buses can be random, thus random access is required for the reduction.

2) *Jacobian matrix assembly*: There are multiple ways to assemble the sparse Jacobian matrix from elements. This step is also a "reduction" because multiple non-zero values for the same location need to be reduced into one by summation. The quickest implementation is to convert the coordinates-value triplets to a new sparse matrix. Due to memory allocation and sorting, this method is usually the slowest.

Alternatively, one can pre-build the sparsity pattern matrix as in the \mathbf{Y}_{bus} method and copy-add elements to the non-zero

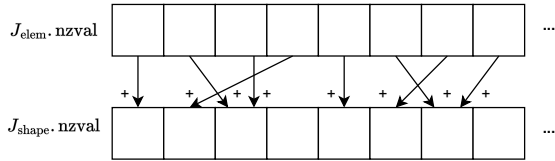


Fig. 2. Copy-adding non-zero elements to the sparsity pattern storage.

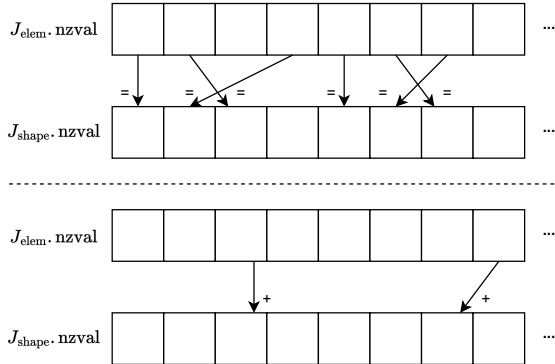


Fig. 3. Two-step technique with separate copying and copy-adding.

array of the sparsity pattern matrix. Fig. 2 illustrates this process, where each element in $\mathbf{J}_{\text{elem}}.\text{nzval}$ require four operations for an element in $\mathbf{J}_{\text{shape}}.\text{nzval}$. These four operations include two loads, one add, and one store.

We propose a two-step implementation technique to separate the initial copy-only operations from subsequent copy-add operations. The two steps are illustrated in Fig. 3. The first step will copy elements from $\mathbf{J}_{\text{elem}}.\text{nzval}$ only when the destinations in $\mathbf{J}_{\text{shape}}.\text{nzval}$ are visited for the first time. It reduces the operations in the first step to one load and one store. Subsequent copy-add operations will cover the remaining elements, which will require four operations. This method eliminates one load and one add operation for $\text{length}(\mathbf{J}_{\text{shape}}.\text{nzval})$ times. Given the reduced memory access, the total time will be considerably reduced. Still, the reduction step has no parallelism and can be more time-consuming than the equation evaluation.

V. CASE STUDIES

This section presents comprehensive benchmark studies on the two methods for a variety of power grid test cases, ranging from 14 to 82,000 buses and more [15]. Micro-benchmarks are first shown to demonstrate the performance gains by the techniques described in Section IV. Next, the \mathbf{Y}_{bus} and the element-wise methods are benchmarked for grid test cases to identify the top performer, analyze the time breakdown, and understand the limitations. Further, multiple x86 and ARM-based computer systems are utilized to understand the trend of scalability as computer systems evolve.

All the discussed algorithms are implemented and optimized in Julia. As a compiled language, Julia provides superior performance for code that is optimally implemented. Generated machine code is inspected to guarantee SIMD vectorization whenever possible. All floating point numbers are stored in

the 64-bit, IEEE 754-compliant format. For complex numbers, the real and imaginary parts are stored using 64 bits.

A. Micro-benchmarks of Computation Steps

This section uses the Synthetic USA system with 82,000 buses on a computer with Intel Core i9-12900K and 3600 MHz DDR4 RAM. The tested 12900K CPU only supports AVX2, which is a 256-bit wide SIMD instruction.

1) \mathbf{Y}_{bus} method: The time to compute power injections is first measured. Specifically, the power injections computation contains two steps: a) phasor calculations and b) sparse matrix and vector calculations, which include steps 2 and 3 in Section IV.B. Cases are compared with the real and imaginary parts of complex phasors stored interleaved or separately. As shown in Table I, separate storage reduces the time to update the voltage vectors by using SIMD, although extra time is required to change the data structure before the power calculations. Note that the best time performance is given in the bold text in all subsequent tables.

TABLE I
P/Q CALCULATION TIME IN μs FOR \mathbf{Y}_{BUS} WITH DIFFERENT STORAGE

	\mathbf{V} and \mathbf{U} Calc.	Power Calc.	Total Time
Interleave	557	722	1279
Separate	137	806	943

The Jacobian computation has two steps: a) $d\mathbf{S}/d\boldsymbol{\theta}$ and $d\mathbf{S}/d\mathbf{V}_m$ calculation, and b) assembly into \mathbf{J} . For Step a), matrix multiplication and the two-pass method are compared. For Step b), the concatenation and in-place methods are compared. It can be seen that the two-pass method is several times faster than the plain matrix multiplication, and the in-place copy approach is nearly 25 times faster than concatenation. In following comparisons with the element-wise method, the fastest methods will be used.

TABLE II
JACOBIAN CALCULATION AND ASSEMBLY TIME IN μs FOR \mathbf{Y}_{BUS} METHOD

Derivatives Calculation		Matrix Assembly	
Matrix Multiplication	Two-Pass	Concatenation	In-Place Copy
13,263	2,733	15,350	602

2) *Element-wise method*: Both the power injection and Jacobian calculations in the element-wise method has two steps: evaluation and reduction. For power injection calculation, with and without SIMD are tested. Table III shows that with the array-based data structure, the SIMD-enabled case only takes about 1/4 of the time without SIMD. This is expected because the processor supports AVX2, which packs four 64-bit floating-point calculations in one instruction.

TABLE III
ELEMENT-WISE POWER INJECTION COMPUTATION TIME IN μs

Evaluation Methods		Reduction
No SIMD	SIMD	
1,179	299	183

For the Jacobian computation, the evaluation time and the three reduction methods are compared in Table IV. For the reduction part, creating a new matrix is much more expensive than the copy-add and the two-step method. Also, calculating all 1,665,936 Jacobian elements takes merely 848 μs , compared with 1,830 μs for the two-step reduction method. Therefore, the bottleneck for Jacobian computation in the element-wise method is in the reduction.

TABLE IV
ELEMENT-WISE JACOBIAN COMPUTATION TIME μs

Vectorized Evaluation	Reduction Methods		
	New matrix	Copy-add	Two-step
848	13,873	2,025	1,830

3) *Comparing \mathbf{Y}_{bus} and element-wise methods*: The best computation times for both methods are given in Table V. It can be seen that the \mathbf{Y}_{bus} method is slower than the element-wise method for both power injection and Jacobian calculations. Since the theoretical computational complexity is in the same order of magnitude (with the \mathbf{Y}_{bus} method having slightly less calculations), the time difference needs to be investigated at the execution level.

TABLE V
COMPARISON OF BEST COMPUTATION TIME IN μs

	\mathbf{Y}_{bus} Method	Element-wise Method
Power Computation	943	482
Jacobian Computation	3,335	2,678

We use the CPU statistics by the Linux `perf` monitoring tool to compare the element-wise Jacobian evaluation and the two-pass method. Note that the element-wise method has more complexity on paper due to the number of elements, but the two-pass method has multiple jumps. The two functions are executed for 1,000 runs, and the CPU statistics are shown in Table VI. It can be seen that the \mathbf{Y}_{bus} method requires more cache access and has nearly twice the cache miss rate than the element-wise method. Also, the \mathbf{Y}_{bus} method has significantly more branches and much higher branch mispredictions. Therefore, the total number of instructions for the \mathbf{Y}_{bus} method is higher, resulting in more cycles and a longer execution time.

TABLE VI
CPU STATISTICS FOR JACOBIAN CALCULATION

	\mathbf{Y}_{bus} J Calculation	Element-wise J Calculation
Cycles	14,327,078,176	4,577,698,819
Cache Access	828,580,410	581,952,974
Cache Misses	156,647,072	60,248,850
Branches	5,474,516,729	19,537,258
Branch Mispredict.	173,767,459	2,538
Instructions	50,308,631,851	3,690,449,376

B. Benchmark for Multiple Test Cases

This section continues to use Intel 12900K for benchmarking the two methods for nine power grid test cases. Results

are shown in Table VII. For the element-wise method, *a)* the Jacobian reduction is the bottleneck of all its computations. *b)* the power equation evaluation scales nearly linearly to system size. For the \mathbf{Y}_{bus} method, the Jacobian calculation is the bottleneck.

Several observations are made by comparison:

- 1) For small cases such as the 14-bus and the 118-bus systems, the \mathbf{Y}_{bus} method is faster in both power injection and Jacobian calculations. This is because all data are likely in the L1 or L2 cache, and the computation demand is insufficient to sustain the pipeline.
- 2) The effect of pipelining can be seen by comparing the power calculation time for the 118-bus and the 300-bus systems. The two systems are of modest sizes so data can mostly fit into L1 and L2 caches. As the number of buses increases by 2.5x, the calculation time increases by a factor of 2.6 for the \mathbf{Y}_{bus} method. For the element-wise method, the calculation time only increases by 2.1x due to improved pipelining for SIMD.
- 3) The power computation is faster using the element-wise method than the \mathbf{Y}_{bus} method for cases with greater than 300 buses. This is possibly due to cache misses in the \mathbf{Y}_{bus} method when performing sparse matrix-vector multiplication.
- 4) The Jacobian computation is faster using the element-wise method for systems of any size. This is mostly due to the branching and jumping that are unfriendly to pipelining, as discussed in Section V.A.3.

Overall, the element-wise method is faster than \mathbf{Y}_{bus} method for both power injection and Jacobian computations for systems ranging from 300 to 82k buses.

C. Computational Complexity Due to Grid Size

While the element-wise method leads in performance, it is observed that the power and Jacobian calculations for the two methods slow down differently. That is, as the system size increases, the average computational complexity increases by more for some operations than others. We can measure a rough metric coined as the “computation time per bus” for each step. As the grid size increases, cache misses and memory access increase, thus a longer computation time per bus is expected.

To characterize the relative computation performance across systems, we calculate the computation-time-per-bus ratios of all systems to that of the 118-bus system. This ratio is termed the “time-cost ratio”. A time-cost ratio smaller than one means that an operation takes less time per bus to perform, as compared to the 118-bus system. Ratios greater than 1 correspond to super-linear complexity (namely, unfavorable scalability), indicating worsening performance as system size increases. The larger the time-cost ratio, the worse the scalability is.

Results are plotted in Fig. 4, which shows that the \mathbf{Y}_{bus} method has linear scalability up to the 2736-bus system because data are likely in the CPU caches. The element-wise method for power calculation has sub-linear scaling and is thus optimal compared with \mathbf{Y}_{bus} . Further, the Jacobian calculation in the element-wise method has worse scalability than the \mathbf{Y}_{bus} method. If this trend sustains, the \mathbf{Y}_{bus} method can be faster to compute the Jacobian than the element-wise method.

TABLE VII
COMPUTATION TIME FOR THE \mathbf{Y}_{bus} AND THE ELEMENT-WISE METHODS FOR SYSTEMS OF DIFFERENT SIZES.
TIME IS GIVEN IN NANoseconds FOR ROWS 1 AND 2 AND IN MICROSECONDS FOR THE REMAINDER.

Case	\mathbf{Y}_{bus} Method			Element-wise Method				
	Phasor Calc.	Power Calc.	J Calc.	J Red.	Power Calc.	Power Red.	J Calc.	J Red.
case14 (ns)	29.86	93.21	333.37	88.93	59.84	105.69	65.46	87.41
case118 (ns)	207.65	519.15	2,819.56	565.71	537.21	300.17	1,044.30	869.42
case300	0.51	1.37	7.19	1.64	1.18	0.54	2.58	2.04
case1354pegase	2.28	5.94	31.82	8.05	5.66	2.65	12.51	13.29
case2736sp	4.75	12.42	65.87	16.70	9.92	4.56	15.49	23.61
case9241pegase	15.49	79.08	341.35	75.46	45.89	26.72	124.80	248.02
case_ACTIVSg25k	41.77	214.54	818.18	176.18	92.62	49.70	230.34	491.11
case_ACTIVSg70k	117.00	665.77	2,291.57	504.21	255.39	142.50	686.66	1,536.49
case_SyntheticUSA	137.09	806.48	2,733.15	602.55	299.40	183.85	847.68	1,829.67

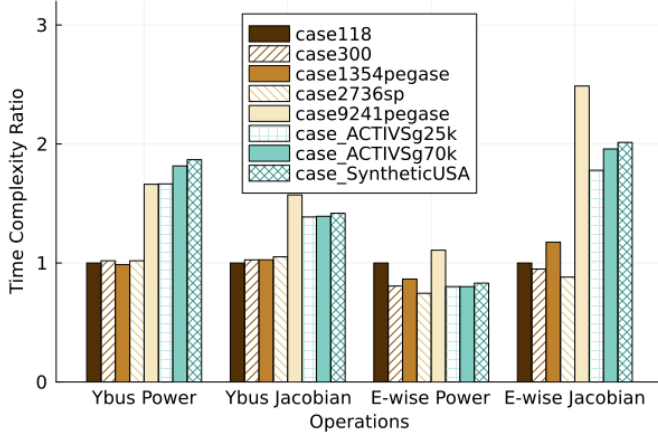


Fig. 4. Time complexity ratio relative to the 118-bus system on 12900K

D. Impact of SIMD Width

As noted, the tested 12900K CPU only supports AVX2, which is 256-bit wide. It is anticipated that CPUs with AVX512 support will be faster for the element-wise evaluations. But is it the case across the board?

We benchmark the nine cases on an Intel 11900K CPU with 32GB DDR4 memory clocking at 3200 MHz. Compared with 12900K, this CPU is one generation older in architecture, runs at a lower frequency, and has smaller caches. Also, the memory is slower than that used in the 12900K system. On the contrary, this CPU supports 512-bit wide SIMD through AVX512. Comparing the results shown in Table VIII with Table VII, the following observations are made:

- 1) Phasor evaluation in the \mathbf{Y}_{bus} method and the power evaluation in the element-wise method is faster for all systems due to AVX512 support. Given the system size, the operands can fit into the L2 cache. These evaluations are thus CPU-bound.
- 2) In the \mathbf{Y}_{bus} method, the power evaluation cannot utilize AVX512. Its computation performance is thus slower and proportional to the CPU clock frequency.
- 3) In the element-wise method, the Jacobian evaluation is faster for small systems and slower for larger ones. The slowdown is due to memory access for large systems. Therefore, this evaluation switches from CPU-bound to memory-bound as system size increases.

It can be concluded that AVX512 will reduce the computation time for vectorized evaluations by a modest percentage, and it is most conducive to small and medium-sized systems. For large systems, the whole computation becomes memory-bound for both methods.

E. Impact of Improved Memory Speed

At this point, it is understood that memory access is the bottleneck for large-scale system calculations. Solutions from computer systems are to clock up the memory and physically move the processor and memory closer. A notable system is the Apple Silicon, which places the RAM beside the processor. This design has the benefit of reduced memory latency, which may lead to performance gains for large-scale systems. Understanding how this design impacts the performance of the two methods will help us to predict their scalability.

Table IX shows the benchmark results on an Apple M2 system with 24 GB LPDDR5 RAM running at 6400 MHz. Apple M2 has support for 128-bit SIMD, 192 KB L1 cache, and 16 MB L2 cache. Comparing Table IX with Table VII provides interesting observations:

- 1) The phasor calculation using \mathbf{Y}_{bus} and the power and Jacobian evaluation using the element-wise method on Apple M2 is consistently within 2x the time of Intel 12900K. This is because these computations are CPU-bound, in which the SIMD width plays a central role.
- 2) The power evaluation in \mathbf{Y}_{bus} is initially slower and later faster on M2 than on 12900K. This is because, for small systems, the larger cache in 12900K can help reduce cache misses. For large systems, the problem will become memory-bound, thus M2 becomes faster.
- 3) The Jacobian calculation in \mathbf{Y}_{bus} is slower on M2 than on 12900K by a stable factor. This step cannot utilize SIMD and is impacted by both the CPU frequency and memory speed.
- 4) The Jacobian reduction is initially CPU-bound but quickly becomes memory bound. Faster memory will bring major improvements to this step.

In addition, Fig. 5 shows the time-cost ratio relative to the 118-bus system on M2. It can be seen that for the 82k-bus Synthetic system, the element-wise method scales slightly worse than the \mathbf{Y}_{bus} method for Jacobian calculation. This observation matches that on the Intel platform, although the

TABLE VIII
BENCHMARK ON INTEL I9-11900K WITH AVX512

Case	Ybus Method				Element-wise Method			
	Phasor Calc.	Power Calc.	J Calc.	J Red.	Power Calc.	Power Red.	J Calc.	J Red.
case14 (ns)	17.46	123.93	463.99	111.28	56.24	145.56	71.34	90.59
case118 (ns)	122.71	605.35	3,911.88	819.61	400.09	443.47	824.30	1,027.40
case300	0.30	1.66	10.06	2.20	0.72	0.78	1.93	2.43
case1354pegase	1.38	6.89	43.85	9.63	3.39	3.57	10.86	19.00
case2736sp	2.72	14.90	91.93	21.79	6.18	6.31	18.64	32.99
case9241pegase	9.41	88.23	430.85	89.32	29.63	34.76	97.57	255.11
case_ACTIVSg25k	25.40	249.08	1,053.98	205.37	58.59	65.77	195.06	394.81
case_ACTIVSg70k	69.62	757.26	3,274.72	712.65	168.35	185.77	755.40	2,041.78
case_SyntheticUSA	81.58	969.50	3,956.52	875.01	205.78	218.37	959.30	2,444.29

TABLE IX
BENCHMARK ON APPLE M2

Case	Ybus Method				Element-wise Method			
	Phasor Calc.	Power Calc.	J Calc.	J Red.	Power Calc.	Power Red.	J Calc.	J Red.
case14 (ns)	42.17	131.38	360.44	100.81	92.32	184.30	93.86	140.80
case118 (ns)	281.18	666.93	2,916.67	761.69	823.96	529.02	688.47	1,366.60
case300	0.69	1.49	7.33	1.86	1.95	0.98	1.75	3.47
case1354pegase	3.12	7.38	34.88	8.58	9.33	5.11	14.29	23.33
case2736sp	6.29	14.71	77.46	17.67	16.42	7.79	18.17	32.75
case9241pegase	21.13	88.42	355.29	69.13	95.33	48.83	124.08	222.04
case_ACTIVSg25k	57.13	227.29	883.04	157.33	190.25	89.17	229.67	332.88
case_ACTIVSg70k	160.08	645.92	2,592.08	452.63	521.21	250.63	1,025.92	962.33
case_SyntheticUSA	187.79	769.29	2,821.54	524.63	619.17	296.88	1,351.75	1,194.46

TABLE X
COMPUTATION TIME IN MICROSECONDS USING ULTRA-LARGE GRID TEST CASES ON INTEL 12900K

Case	Ybus Method				Element-wise Method			
	Phasor Calc.	Power Calc.	J Calc.	J Red.	Power Calc.	Power Red.	J Calc.	J Red.
164k	275	1,721	5,806	1,478	608	373	2,084	4,192
246k	412	2,796	9,043	2,580	937	583	3,344	7,369
328k	549	4,060	12,511	3,938	1,346	775	4,577	11,067
410k	689	5,208	15,948	5,300	1,915	965	6,008	16,740

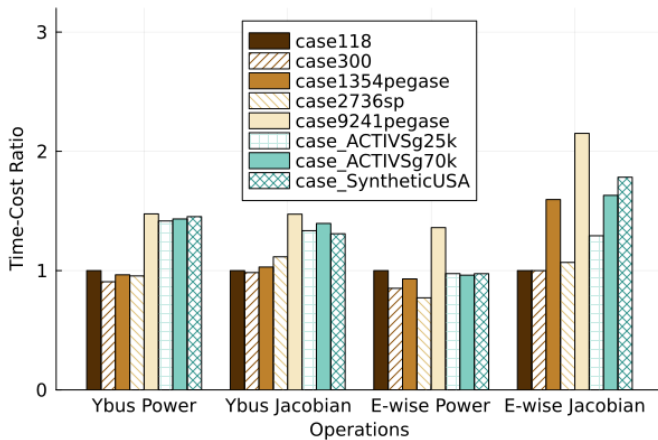


Fig. 5. Computation time ratio relative to the 118-bus system on Apple M2

gap becomes smaller since faster memory is more helpful to the element-wise method.

F. Outlook for Ultra-Large Systems

The tested cases with up to 82k buses declare the element-wise method as a winner for large-scale systems. Still, worse scalability is observed for the Jacobian computation in the element-wise method. This indicates that, as the system size further increases, the \mathbf{Y}_{bus} method may take over. This section investigates how the two methods will continue to scale for ultra-large cases to understand the performance turning points.

The 82k-bus Synthetic USA system is repeated multiple times to create four ultra-large systems. All buses and lines are duplicated by two to five times, respectively, resulting in four cases. The performance of the two methods on 12900K and Apple M2 are reported in Table X and Table XI. It can be seen that the Jacobian reduction step in the element-wise method continues to scale poorly. On the Intel platform, the \mathbf{Y}_{bus} method and the element-wise methods will be similarly slow when the number of buses reaches about 328k. On the M2 platform, the tie happens around 246k buses.

Regarding the question that which of the two methods will be faster on future systems, we argue that the element-wise method will continue to outperform the \mathbf{Y}_{bus} method for large-scale systems ranging from 1k to 410k buses or more. If

TABLE XI
COMPUTATION TIME IN MICROSECONDS USING ULTRA-LARGE GRID TEST CASES ON APPLE M2

Case	Ybus Method				Element-wise Method			
	Phasor Calc.	Power Calc.	J Calc.	J Red.	Power Calc.	Power Red.	J Calc.	J Red.
164k	367	1,698	5,911	1,158	1,256	594	2,906	3,442
246k	566	2,577	8,883	1,776	1,930	912	4,771	6,414
328k	757	3,435	12,079	2,399	2,619	1,226	6,953	9,590
410k	950	4,350	15,096	3,006	3,226	1,538	7,982	12,798

we take the best columns from Table X and Table XI, the element-wise method is a clear winner for power calculation. For the Jacobian calculation, the best columns of the two methods will take roughly the same time for the 410k bus system. Nevertheless, faster memory and AVX2/AVX512 will moderately benefit the element-wise Jacobian calculation but not as much for the \mathbf{Y}_{bus} method. In addition, the Jacobian reduction method presented in Section IV still has room for optimization, but that is beyond the scope of this paper.

VI. CONCLUSIONS

In this paper, we investigated the computational performance of the \mathbf{Y}_{bus} method for power injection calculation and sparse Jacobian formulation. The main findings are as follows:

- 1) The major issue with the \mathbf{Y}_{bus} method is the sparse matrix-centered computations, which are not capable of utilizing SIMD and incurs many jumps due to indexing.
- 2) Compared with the element-wise method, the \mathbf{Y}_{bus} method is slower for practical systems with bus numbers ranging from thousands to a few hundred thousand on the x86 CPUs.
- 3) The bottleneck for the element-wise method is reducing the Jacobian elements into a sparse matrix. The step scales poorly as the number of buses enters the realm of hundreds of thousands. This step is primarily constrained by memory speed.

We conclude that the \mathbf{Y}_{bus} method trails the element-wise method for practical power grids on modern computers, especially those with wide SIMD support and fast memory. Bus admittance matrix, as a network reduction method for increasing computation performance, is missing the support for new processor features due to its computational irregularity. Future work needs to investigate algorithms for reducing the time complexity of the Jacobian reduction step in the element-wise method.

REFERENCES

- [1] W. F. Tinney and C. E. Hart, "Power Flow Solution by Newton's Method," *IEEE Transactions on Power Apparatus and Systems*, vol. PAS-86, no. 11, pp. 1449–1460, Nov. 1967, ISSN: 0018-9510. DOI: 10.1109/TPAS.1967.291823.
- [2] W. F. Tinney, "Compensation Methods for Network Solutions by Optimally Ordered Triangular Factorization," *IEEE Transactions on Power Apparatus and Systems*, vol. PAS-91, no. 1, pp. 123–127, Jan. 1972, ISSN: 0018-9510. DOI: 10.1109/TPAS.1972.293321.
- [3] P. E. Ross. (Apr. 1, 2008). "Why CPU Frequency Stalled," *IEEE Spectrum*, [Online]. Available: <https://spectrum.ieee.org/why-cpu-frequency-stalled> (visited on 03/20/2022).
- [4] D. Kirk and W.-m. Hwu, *Programming Massively Parallel Processors: A Hands-on Approach*, Third edition. Amsterdam ; Cambridge, MA: Elsevier, 2017, 550 pp., ISBN: 978-0-12-811986-0.
- [5] D. Etiemble, *45-year CPU evolution: One law and two equations*, Mar. 1, 2018. DOI: 10.48550/arXiv.1803.00254. arXiv: 1803.00254 [cs]. [Online]. Available: <http://arxiv.org/abs/1803.00254> (visited on 11/22/2022).
- [6] M. J. Flynn and K. W. Rudd, "Parallel architectures," *ACM Computing Surveys*, vol. 28, no. 1, p. 4, 1996.
- [7] H. Cui, F. Li, and K. Tomsovic, "Hybrid Symbolic-Numeric Framework for Power System Modeling and Analysis," *IEEE Transactions on Power Systems*, vol. 36, no. 2, Mar. 2021, ISSN: 1558-0679. DOI: 10.1109/TPWRS.2020.3017019.
- [8] F. Milano, "Power System Modelling and Scripting," in *Power System Modelling and Scripting*, ser. Power Systems, F. Milano, Ed., Berlin, Heidelberg: Springer, 2010, pp. 3–17.
- [9] F. Milano, "An open source power system analysis toolbox," *IEEE Transactions on Power Systems*, vol. 20, no. 3, pp. 1199–1206, Aug. 2005, ISSN: 1558-0679. DOI: 10.1109/TPWRS.2005.851911.
- [10] J. H. Chow and J. J. Sanchez-Gasca, *Power System Modeling, Computation, and Control*. John Wiley & Sons, Jan. 21, 2020, 664 pp., ISBN: 978-1-119-54687-0. Google Books: M8G_DwAAQBAJ.
- [11] J. D. Glover, T. J. Overbye, M. S. Sarma, and A. Birchfield, *Power System Analysis and Design*. Cengage Learning, 2022.
- [12] T. A. Davis and E. P. Natarajan, *User Guide for KLU and BTF*, 2022.
- [13] F. Schäfer and M. Braun, "An efficient open-source implementation to compute the jacobian matrix for the Newton-Raphson power flow algorithm," in *2018 IEEE PES Innovative Smart Grid Technologies Conference Europe (ISGT-Europe)*, Oct. 2018, pp. 1–6. DOI: 10.1109/ISGTEurope.2018.8571471.
- [14] S. P. Vera, *SanPen/GridCal*: Zenodo, Jul. 24, 2022. DOI: 10.5281/zenodo.6896466. [Online]. Available: <https://zenodo.org/record/6896466> (visited on 11/23/2022).
- [15] R. D. Zimmerman, C. E. Murillo-Sánchez, and R. J. Thomas, "MATPOWER: Steady-State Operations, Planning, and Analysis Tools for Power Systems Research and Education," *IEEE Transactions on Power Systems*, vol. 26, no. 1, pp. 12–19, Feb. 2011. DOI: 10.1109/TPWRS.2010.2051168.